Acta Astronautica 93 (2014) 509–515

Contents lists available at ScienceDirect

Acta Astronautica

journal homepage: www.elsevier.com/locate/actaastro

MESSENGER at Mercury: Early orbital operations

Ralph L. McNutt Jr.[a,*], Sean C. Solomon[b], Peter D. Bedini[a], Brian J. Anderson[a], David T. Blewett[a], Larry G. Evans[c], Robert E. Gold[a], Stamatios M. Krimigis[a,d], Scott L. Murchie[a], Larry R. Nittler[b], Roger J. Phillips[e], Louise M. Prockter[a], James A. Slavin[f], Maria T. Zuber[g], Eric J. Finnegan[a], David G. Grant[a], the MESSENGER Team

[a] The Johns Hopkins University Applied Physics Laboratory, Laurel, MD 20723, USA
[b] Department of Terrestrial Magnetism, Carnegie Institution of Washington, Washington, DC 20015, USA
[c] Computer Sciences Corporation, Lanham-Seabrook, MD 20706, USA
[d] Academy of Athens, Athens 11527, Greece
[e] Southwest Research Institute, Boulder, CO 80302, USA
[f] Heliophysics Science Division, NASA Goddard Space Flight Center, Greenbelt, MD 20771, USA
[g] Department of Earth, Atmospheric and Planetary Sciences, MIT, Cambridge, MA 02129, USA

ARTICLE INFO

Article history:
Received 11 January 2012
Accepted 8 August 2012
Available online 16 November 2012

Keywords:
Mercury
MESSENGER
Planetary science
Orbital missions
NASA
Surface composition
Exosphere
Impact basins
Gravity field

ABSTRACT

The MErcury Surface, Space ENvironment, GEochemistry, and Ranging (MESSENGER) spacecraft, launched in August 2004 under NASA's Discovery Program, was inserted into orbit about the planet Mercury in March 2011. MESSENGER's three flybys of Mercury in 2008–2009 marked the first spacecraft visits to the innermost planet since the Mariner 10 flybys in 1974–1975. The unprecedented orbital operations are yielding new insights into the nature and evolution of Mercury. The scientific questions that frame the MESSENGER mission led to the mission measurement objectives to be achieved by the seven payload instruments and the radio science experiment. Interweaving the full set of required orbital observations in a manner that maximizes the opportunity to satisfy all mission objectives and yet meet stringent spacecraft pointing and thermal constraints was a complex optimization problem that was solved with a software tool that simulates science observations and tracks progress toward meeting each objective. The final orbital observation plan, the outcome of that optimization process, meets all mission objectives. MESSENGER's Mercury Dual Imaging System is acquiring a global monochromatic image mosaic at better than 90% coverage and at least 250 m average resolution, a global color image mosaic at better than 90% coverage and at least 1 km average resolution, and global stereo imaging at better than 80% coverage and at least 250 m average resolution. Higher-resolution images are also being acquired of targeted areas. The elemental remote sensing instruments, including the Gamma-Ray and Neutron Spectrometer and the X-Ray Spectrometer, are being operated nearly continuously and will establish the average surface abundances of most major elements. The Visible and Infrared Spectrograph channel of MESSENGER's Mercury Atmospheric and Surface Composition Spectrometer is acquiring a global map of spectral reflectance from 300 to 1450 nm wavelength at a range of incidence and emission angles. Targeted areas have been selected for spectral coverage into the ultraviolet with the Ultraviolet and Visible Spectrometer (UVVS). MESSENGER's Mercury Laser Altimeter is acquiring topographic profiles when the slant range to Mercury's surface is less than 1800 km, encompassing latitudes from 20°S to the north pole. Topography over the remainder of

* Corresponding author. Tel.: +1 443 778 5435; fax: +1 443 778 0386.
E-mail address: ralph.mcnutt@jhuapl.edu (R.L. McNutt Jr.).

0094-5765/$ - see front matter © 2012 IAA. Published by Elsevier Ltd. All rights reserved.
http://dx.doi.org/10.1016/j.actaastro.2012.08.012

the southern hemisphere will be derived from stereo imaging, radio occultations, and limb profiles. MESSENGER's radio science experiment is determining Mercury's gravity field from Doppler signals acquired during frequent downlinks. MESSENGER's Magnetometer is measuring the vector magnetic field both within Mercury's magnetosphere and in Mercury's solar wind environment at an instrument sampling rate of up to 20 samples/s. The UVVS is determining the three-dimensional, time-dependent distribution of Mercury's exospheric neutral and ionic species via their emission lines. During each spacecraft orbit, the Energetic Particle Spectrometer measures energetic electrons and ions, and the Fast Imaging Plasma Spectrometer measures the energies and mass per charge of thermal plasma components, both within Mercury's magnetosphere and in Mercury's solar-wind environment. The primary mission observation sequence will continue for one Earth year, until March 2012. An extended mission, currently under discussion with NASA, would add a second year of orbital observations targeting a set of focused follow-on questions that build on observations to date and take advantage of the more active Sun expected during 2012–2013. MESSENGER's total primary mission cost, projected at $446 M in real-year dollars, is comparable to that of Mariner 10 after adjustment for inflation.

© 2012 IAA. Published by Elsevier Ltd. All rights reserved.

1. Introduction

1.1. Background

The MErcury Surface, Space ENvironment, GEochemistry, and Ranging (MESSENGER) [1] spacecraft was launched in August 2004 [2] as the seventh mission in NASA's Discovery Program. Following the trajectory design, MESSENGER completed six planetary flybys, including one of Earth, two of Venus [3], and three of Mercury [4]. The flybys enabled a full checkout of the scientific payload, and the data collected have led to substantial advances in understanding Mercury, beyond the discoveries of Mariner 10.

MESSENGER's primary mission remains centered on 1 year of orbital observations from a nominal 12-h orbit, initially with a periapsis altitude of 200 km, an inclination of 82.5°, and a periapsis latitude of 60°N. These orbital parameters were carefully chosen to comply with propellant and trajectory constraints, thermal and power requirements, and the science plan defined by the Program Level Requirements (PLR) for the MESSENGER project.

The MESSENGER spacecraft will accomplish its scientific investigations with its payload of seven science instruments plus the telecommunication system for radio science (RS) [5]. The instruments include the Mercury Dual Imaging System (MDIS), which consists of an 11-color-filter wide-angle camera (WAC) and a panchromatic narrow-angle camera (NAC) mounted on a single-degree-of-freedom scan platform [6]; a Gamma-Ray and Neutron Spectrometer (GRNS), including Gamma-Ray Spectrometer (GRS) and Neutron Spectrometer (NS) sensors [7]; an X-Ray Spectrometer (XRS), including sensors that point at the planet and at the Sun [8]; a Magnetometer (MAG) [9]; the Mercury Laser Altimeter (MLA) [10]; the Mercury Atmospheric and Surface Composition Spectrometer (MASCS), which uses a common telescope for the Ultraviolet and Visible Spectrometer (UVVS) and the Visible and Infrared Spectrograph (VIRS) [11]; and an Energetic Particle and Plasma Spectrometer (EPPS), consisting of the Energetic Particle Spectrometer (EPS) and the Fast Imaging Plasma Spectrometer (FIPS) [12].

1.2. Accomplishments: discoveries from the Mercury flybys

In addition to providing key gravity assists that enabled orbit insertion and opportunities to test science operations and command sequences for all payload instruments, MESSENGER's three flybys of Mercury yielded a number of discoveries that changed our view of Mercury and influenced preparations for orbital operations.

Regarding Mercury's geological history, MESSENGER established that:

- Volcanism was widespread on Mercury and extended from before the end of heavy bombardment to the second half of solar system history [13–16].
- Mercury experienced pyroclastic volcanism, indicating that interior volatile contents were at least locally much higher than previously thought [13,17].
- Impact crater formation excavated material compositionally distinct from surrounding terrain, providing a means to probe composition versus depth [18–20].
- Contraction spanned much of Mercury's geological history [21–23].
- Large impact basins on Mercury were foci for concentrated magmatic activity and diverse styles of deformation [16,24,25].

Regarding the composition of Mercury's surface and surface-derived exosphere, MESSENGER demonstrated that:

- Mercury's surface silicates, even in fresh crater ejecta, contain little or no FeO [26,27].
- Mercury's thermal neutron flux matches that of several lunar maria, indicating that Fe and Ti are present in comparable abundances, perhaps as oxides [28].
- Mg and Ca^+ are present in Mercury's exosphere [29,30].
- Mercury's comet-like neutral tail contains multiple species [29–31].
- Mg, Ca, and Na have distinct distributions in the exosphere and tail, indicating species-dependent and time-variable source, transfer, and loss processes [29–32].

Regarding Mercury's internal structure and dynamics, MESSENGER showed that:

- The equatorial topographic relief of Mercury, in agreement with earlier radar results, is at least 5.5 km [33].
- Mercury's long-wavelength equatorial topography is well fit by an ellipse aligned with the equatorial ellipticity of the gravity field [34].
- The case for a liquid outer core on Mercury is greatly strengthened [34].
- Mercury's internal magnetic field is dominantly dipolar with a vector moment closely aligned with the spin axis [35–37].

Regarding magnetospheric dynamics at Mercury, MESSENGER established that:

- Mercury's magnetosphere is more responsive to interplanetary magnetic field (IMF) fluctuations than those of other planets [38–40].
- Under southward IMF, rates of magnetic reconnection are ~10 times typical rates at Earth [39].
- Loading of magnetic flux from the dayside magnetosphere to the magnetotail and substorm-like unloading occur at timescales (minutes) much shorter than at Earth (hours), but no energetic particles have been observed to date [40].
- Loading can be so intense that much of Mercury's dayside surface could be directly exposed to the shocked solar wind of the magnetosheath [40].

2. Primary mission objectives

The MESSENGER spacecraft is orbiting Mercury in the geometry shown in Fig. 1. The nominal 12-h orbit is approximately fixed in inertial space so that the orbit completes a local-time rotation once every Mercury orbital period of 88 days. One 8-h Deep Space Network (DSN) downlink is scheduled every day, and the phasing of the downlink relative to apoapsis is chosen to maximize time available for viewing the illuminated planet. During every 88 days, there are two dawn-dusk orbit seasons, one long-eclipse season, and one short-eclipse season. The long-eclipse seasons, when the ascending node of the orbit is in the planet's shadow, are the most stressful to the spacecraft power and thermal systems because, in addition to long-eclipse windows, the spacecraft passes at low altitude over the subsolar region of the planet. The solar flux at Mercury is up to 11 times higher than at Earth, so the spacecraft sunshade always faces the Sun to within a $12^\circ \times 10^\circ$ angular Sun-keep-in (SKI) boundary relative to the center of the sunshade. The back of the spacecraft is exposed to radiant heat from the planet, but the elliptical orbit minimizes the time spent at low altitudes over the hot planet and allows the spacecraft to re-radiate heat at high altitudes. Because one solar day at Mercury equals 176 Earth days, the 1-year primary orbital mission spans only two Mercury solar days. The surface mapping observations were therefore pre-planned for the entire year to ensure coverage of the full planet under optimized illumination and viewing geometries. The highest-priority imaging observations are scheduled for the first solar day, so that any missed observations can be recovered during the second solar day. Topography, surface composition, RS, exosphere, and magnetosphere observation campaigns are coordinated to ensure that each investigation acquires the data required for its respective objectives. The MDIS cameras are mounted on a pivot that provides freedom to view sunward and anti-sunward of the common instrument boresight direction, and the majority of the MDIS observations are acquired while spacecraft pointing is dedicated to one of the other instruments.

2.1. Expected geology results from the primary science mission

The geology investigations address science questions by means of crosscutting campaigns with MDIS and MASCS, as well as information provided by MLA, XRS, MAG, and GRNS. MDIS is acquiring three global mosaics: (1) a cartographic mosaic of monochromatic images obtained viewing nadir to characterize the distribution and stratigraphy of landforms and geological units; (2) a

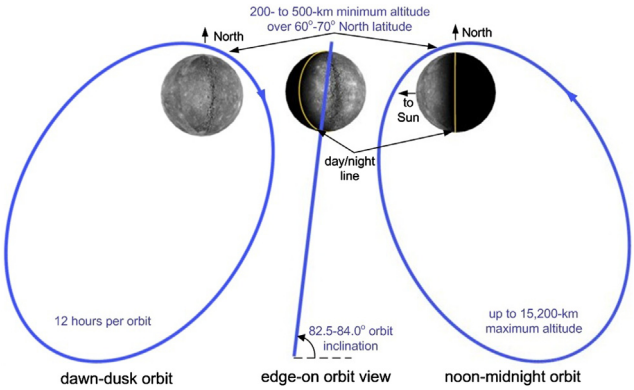

Fig. 1. Geometry of MESSENGER's orbit about Mercury. The orbit is highly eccentric, with the spacecraft passing 200 km above the surface at periapsis and at 15,200 km altitude at apoapsis. At the start of the orbital mission, the orbit plane is inclined 82.5° to Mercury's equator, and the lowest point in the orbit is reached at 60°N latitude. The orbit inclination is expected to drift to 84° over one Earth-year. The periapsis altitude drifts upward, so episodic orbit-correction maneuvers are used to bring the periapsis altitude back down to 200 km.

stereo complement of the monochromatic mosaic to determine the forms of volcanic constructs, tectonic features, and craters; and (3) a multispectral mosaic covering 395- to 1040-nm wavelength to characterize surface materials. Targeted observations provide increased resolution of key features identified from prior observations and special measurement sets that require specific pointing (e.g., photometric function characterizations). MDIS is also acquiring repeated images of the south pole to map permanently shadowed regions and an orchestrated set of limb images of the southern hemisphere to constrain long-wavelength topography.

MASCS is obtaining global maps of spectral reflectance over the wavelengths 300–1450 nm and targeted observations at wavelengths of 115–1450 nm. These measurements provide information about the types of minerals on Mercury's surface, their compositions (e.g., FeO contents of mafic silicates), and their correlation with specific geological units. VIRS is acquiring spectra along strips as the spacecraft motion moves the instrument field of view across the surface. Unlike VIRS, UVVS does not acquire all wavelengths simultaneously, so its targeted surface measurements are obtained by sustained pointing at high-priority locations.

MLA is providing topographic profiles across a variety of geological features in the northern hemisphere that will enable their morphometric characteristics to be determined. XRS and GRNS are helping to constrain the compositions of geological terrains, and MAG is determining whether crustal magnetic anomalies are present. These complementary instruments acquire globally distributed measurements for which resolution is strongly dependent on spacecraft altitude.

2.2. Expected geochemistry results from the primary science mission

Several instruments provide compositional measurements of Mercury's surface. From global color images acquired with MDIS, geological units and features with distinct spectral properties and hence mineralogical compositions are being identified.

GRS is providing global and regional-scale abundance measurements of a number of important elements, including Fe, Mg, Si, Ti, Ca, K, and Th. NS is providing constraints on chemical abundances through the capacity of the elemental constituents of the regolith (such as Fe, Ti, Gd, and Sm) to absorb thermal neutrons. It also provides a measure of the mean atomic mass of elements in the regolith. XRS is providing abundances of Mg, Al, Si, S, Ca, Ti, and Fe.

GRS, NS, and XRS depend critically on counting statistics. Elements for which count rates are low require summing data over broad areas to accumulate sufficient statistics, and thus the spatial resolution varies among elements. For XRS, the detection of the important elements S, Ca, Ti, and Fe depends on the enhanced solar X-ray flux during flares. The high signal during flares provides some degree of enhanced spatial resolution as well, but because of the unpredictable timing of flares, specific regions of the planet are not targeted for such observations.

2.3. Expected geophysics results from the primary science mission

The MLA, MAG, and MDIS instruments and the RS experiment are yielding data for the geophysics investigations. Magnetic field data are acquired continuously and record the planetary magnetic field and signatures of magnetospheric structure and boundaries. The RS experiment is providing range-rate data between the spacecraft and DSN ground stations from which we derive, and periodically update, a spherical harmonic expansion of Mercury's gravity field. Doppler tracking data are acquired on every downlink pass and through every periapsis pass on downlink orbits. The spacecraft radio frequency (RF)

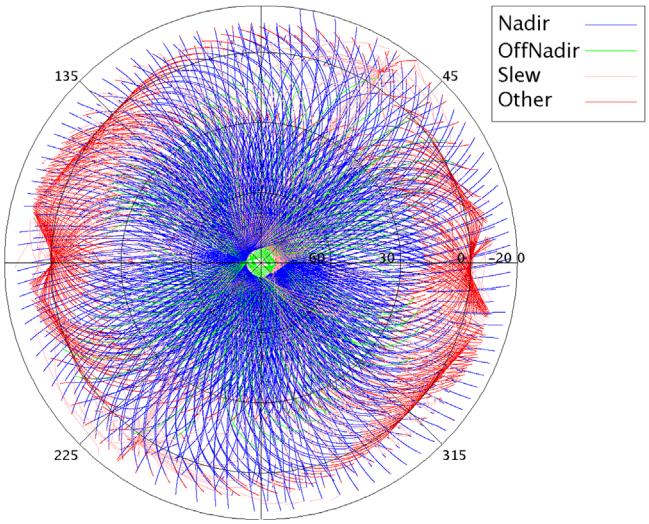

Fig. 2. MLA coverage during the primary science mission in a north polar view for latitudes from 90°N to 20°S.

system operates continuously in orbit to maximize the utility of additional DSN coverage.

In orbit, MLA measures the line-of-sight distance to the surface at ranges of ≤ 1200 km with $>90\%$ detection probability. Ranging is conducted up to 1800 km with somewhat reduced detection probability to map nearly the entire northern hemisphere and from the equator to 20°S (Fig. 2). Profiles have an along-track resolution of 0.8–1 km and a vertical precision <1 m.

The RF tracking data give precise occultation entry and exit times when Mercury blocks the spacecraft as viewed from Earth (Fig. 3). The RF tracking plan ensures that at least half of these events are tracked. The occultation times constrain the planetary radius at the location of the grazing path [41] to an accuracy of ~ 100 m. Measurements in the southern hemisphere are particularly important because MLA does not acquire range data south of 20°S. MDIS observations include limb imaging, which provides additional constraints on planetary shape and topography.

Mercury's internal structure can be derived from the planet's gravity field and shape. The obliquity and forced libration amplitude were estimated from Earth-based radar data [42], and independent estimates will be derived from MESSENGER [43]. The radial density structure of Mercury can be constrained by the dimensionless polar moment of inertia, C/MR^2, where M is Mercury's mass and R is Mercury's radius, given the second-degree and -order coefficients in the spherical harmonic expansion of the planet's gravitational potential, C_{20} and C_{22}, together with the planet's obliquity [44].

The observations also constrain the state of the core. The libration amplitude together with the gravity field and the obliquity determine the ratio C_m/C, where C_m is the moment of inertia of Mercury's mantle and crust. C_m/C is <1 only if the outer core is molten [44], as we expect [42]. When combined with the corresponding terms for topography, the coefficients C_{20} and C_{22} provide fundamental information on the distribution of density in the planet. Presently the value of C_{20} remains poorly constrained [34]. Radio tracking during the primary mission will determine C_{20} to $<0.4\%$ and C_{22} to $<1\%$, and the radio tracking and laser altimetry may reduce the current uncertainties in the physical libration amplitude (35.8 ± 2 arcsec) and obliquity (2.11 ± 0.1 arcmin). From the values of C/MR^2 and C_m/C, we can estimate the moment of inertia of the core, C_c. Knowledge of C_c will constrain the radius and density of the solid inner portion of the core.

Structure in the magnetic field can be used to infer the convective state of the liquid core. Current best estimates for Mercury's dipole moment are in the range 240–270 nT–R^3. If we can account for external fields, core field structure in the northern hemisphere can be recovered [36] at wavelengths corresponding to spherical harmonic degree and order 10, allowing discrimination among different classes of core dynamo models [45–47].

2.4. Expected results on Mercury's exosphere and magnetosphere from the primary science mission

During the primary mission, MAG, EPPS, and MASCS are acquiring data nearly continuously to characterize Mercury's magnetosphere and exosphere, yielding the in situ coverage shown in Fig. 4. MAG is obtaining vector measurements of the magnetic field, at a time resolution of 20 samples/s and a field resolution of 0.05 nT, to characterize Mercury's magnetic field and magnetospheric structures, boundaries, and wave processes. The FIPS sensor on EPPS is acquiring wide angular sampling of ions with species discrimination for energies from 50 eV to 20 keV. These data allow identification of boundaries and plasmas within the magnetosphere. The EPS sensor of EPPS monitors higher-energy ions and electrons, from 15 to 1000 keV, to assess the entry of solar energetic particles into the magnetosphere and access to the planetary surface and also to identify magnetospheric acceleration processes inferred from Mariner 10 observations but so far not confirmed by MESSENGER flyby measurements.

The UVVS portion of MASCS is recording emission lines of many neutral and ion species and mapping the distributions of species within the exosphere. Several spacecraft pointing sequences are used to examine different regions. To identify species released from the dayside surface, sets of altitude scans spaced regularly in local solar time and spanning dusk to dawn are executed approximately every other orbit. As a supplement to these observations, UVVS takes data whenever the boresight of the instrument does not intercept the planet, providing numerous scans at varying geometry. To survey the higher altitudes and near-tail region, scans are performed whenever the spacecraft is above 5000-km altitude and the $+Z$-axis of the spacecraft cannot be pointed to the

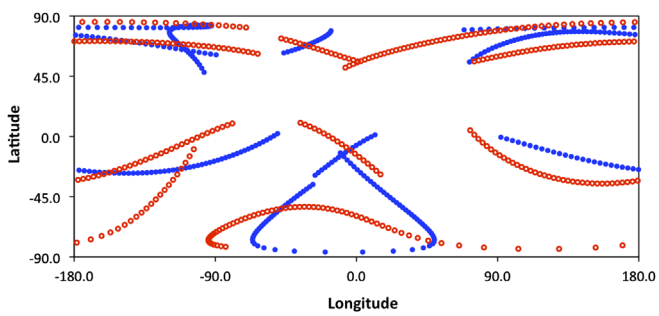

Fig. 3. Occultation points during the primary mission. Red indicates ingress, and blue indicates egress.

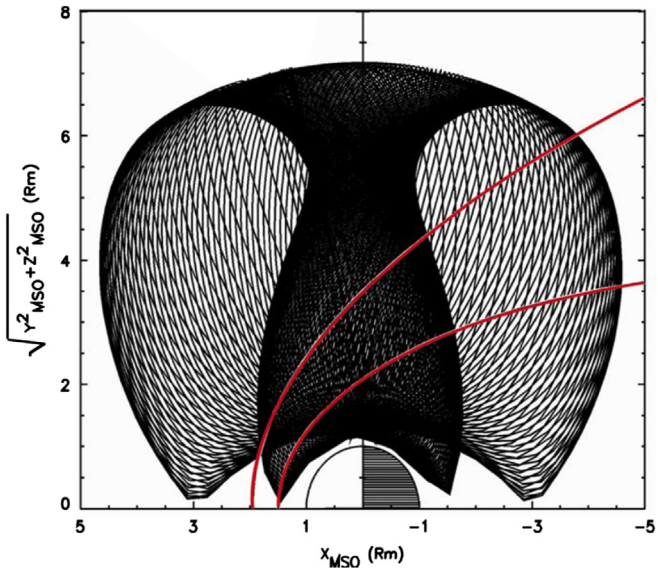

Fig. 4. Coverage of the magnetosphere represented by MESSENGER's orbital trajectory during the primary mission in Mercury solar orbital (MSO) coordinates (X_{MSO} is to the Sun, Z_{MSO} is northward, and Y_{MSO} is positive duskward). Orbits are shown in black projected onto the X_{MSO}-$\sqrt{(Y^2+Z^2)}$ plane. The traces in red are the expected mean locations of the magnetopause (inner) and bow shock (outer) surfaces in the $X_{MSO}=0$ plane.

planetary surface. On selected orbits, the spacecraft scans to point UVVS across the northern and then southern polar regions to survey volatiles coming from the poles.

3. Summary

Following six and a half years of cruise, calibration, and scientific observations during three flybys of Mercury, MESSENGER is now in orbit about the innermost planet. After spacecraft and instrument checkout from orbit, the first systematic orbital scientific observations of Mercury began in early April. As has been noted from the time of the initial proposal of this mission to NASA's Discovery Program in December 1996, understanding Mercury and the forces that shaped it is key to our understanding of the formation of the terrestrial planets of our solar system and particularly of Earth. The discovery that hundreds of extrasolar planets are in orbits about their host stars that are comparable in size or smaller than Mercury's orbit about the Sun suggests that detailed understanding of Mercury in our own system may play an important role in developing our understanding of planetary systems in general.

Reaching this point in the mission has not been without technical challenges. However, the three flybys of Mercury have already advanced our understanding of the innermost planet well beyond the state of knowledge following the Mariner 10 encounters more than three decades earlier. Moreover, the MESSENGER spacecraft and payload are healthy, and the team is confident that all program level requirements for the primary mission can be met.

Acknowledgments

The NASA Discovery Program under contract NAS5-97271 to The Johns Hopkins University Applied Physics Laboratory and NASW-00002 to the Carnegie Institution of Washington supports the MESSENGER mission to Mercury.

References

[1] S.C. Solomon, et al., MESSENGER mission overview, Space Sci. Rev. 131 (2007) 3–39.
[2] R.L. McNutt Jr., et al., The MESSENGER mission to Mercury: development history and early mission status, Adv. Space Res. 38 (2006) 564–571.
[3] R.L. McNutt Jr., et al., The MESSENGER mission to Mercury: status after the Venus flybys, Acta Astronaut. 63 (2008) 68–73.
[4] R.L. McNutt Jr., et al., The MESSENGER mission: results from the first two Mercury flybys, Acta Astronaut. 67 (2010) 681–687.
[5] D.K. Srinivasan, et al., The radio frequency subsystem and radio science on the MESSENGER mission, Space Sci. Rev. 131 (2007) 557–571.
[6] S.E. Hawkins III, et al., The Mercury Dual Imaging System on the MESSENGER spacecraft, Space Sci. Rev. 131 (2007) 247–338.
[7] J.O. Goldsten, et al., The MESSENGER Gamma-Ray and Neutron Spectrometer, Space Sci. Rev. 131 (2007) 339–391.
[8] C.E. Schlemm, et al., The X-Ray Spectrometer on the MESSENGER spacecraft, Space Sci. Rev. 131 (2007) 393–415.
[9] B.J. Anderson, et al., The Magnetometer instrument on MESSENGER, Space Sci. Rev. 131 (2007) 417–450.
[10] J.F. Cavanaugh, et al., The Mercury Laser Altimeter instrument for the MESSENGER mission, Space Sci. Rev. 131 (2007) 451–479.
[11] W.E. McClintock, M.R. Lankton, The Mercury Atmospheric and Surface Composition Spectrometer for the MESSENGER mission, Space Sci. Rev. 131 (2007) 481–521.
[12] G.B. Andrews, et al., The Energetic Particle and Plasma Spectrometer instrument on the MESSENGER spacecraft, Space Sci. Rev. 131 (2007) 523–556.
[13] J.W. Head, et al., Volcanism on Mercury: evidence from the first MESSENGER flyby, Science 321 (2008) 69–72.
[14] R.G. Strom, et al., Mercury cratering record viewed from MESSENGER's first flyby, Science 321 (2008) 79–81.

[15] C.I. Fassett, et al., Caloris impact basin: exterior geomorphology, stratigraphy, morphometry, radial sculpture, and smooth plains deposits, Earth Planet. Sci. Lett. 285 (2009) 297–308.
[16] L.M. Prockter, et al., Evidence for young volcanism on Mercury from the third MESSENGER flyby, Science 329 (2010) 668–671.
[17] L. Kerber, et al., Explosive volcanic eruptions on Mercury: eruption conditions, magma volatile content, and implications for interior volatile abundances, Earth Planet. Sci. Lett 285 (2009) 263–271.
[18] M.S. Robinson, et al., Reflectance and color variations on Mercury: Regolith processes and compositional heterogeneity, Science 321 (2008) 66–69.
[19] B.W. Denevi, et al., The evolution of Mercury's crust: a global perspective from MESSENGER, Science 324 (2009) 613–618.
[20] C.M. Ernst, et al., Exposure of spectrally distinct material by impact craters on Mercury: implications for global stratigraphy, Icarus 209 (2010) 210–223.
[21] S.C. Solomon, et al., Return to Mercury: a global perspective on MESSENGER's first Mercury flyby, Science 321 (2008) 59–62.
[22] T.R. Watters, et al., The tectonics of Mercury: the view after MESSENGER's first flyby, Earth Planet. Sci. Lett. 285 (2009) 283–296.
[23] M.T. Zuber, et al., Accommodation of lithospheric shortening on Mercury from altimetric profiles of ridges and lobate scarps measured during MESSENGER flybys 1 and 2, Icarus 209 (2010) 247–255.
[24] S.L. Murchie, et al., Geology of the Caloris basin, Mercury: a view from MESSENGER, Science 321 (2008) 73–76.
[25] T.R. Watters, et al., Evolution of the Rembrandt impact basin on Mercury, Science 324 (2009) 618–621.
[26] W.E. McClintock, et al., Spectroscopic observations of Mercury's surface reflectance during MESSENGER's first Mercury flyby, Science 321 (2008) 62–65.
[27] G.M. Holsclaw, et al., A comparison of the ultraviolet to near-infrared spectral properties of Mercury and the Moon as observed by MESSENGER, Icarus 209 (2010) 179–194.
[28] D.J. Lawrence, et al., Identification and measurement of neutron-absorbing elements on Mercury's surface, Icarus 209 (2010) 195–209.
[29] W.E. McClintock, et al., MESSENGER observations of Mercury's exosphere: detection of magnesium and distribution of constituents, Science 324 (2009) 610–613.
[30] R.J. Vervack Jr., et al., Mercury's complex exosphere: results from MESSENGER's third flyby, Science 329 (2010) 672–675.
[31] W.E. McClintock, et al., Mercury's exosphere: observations during MESSENGER's first Mercury flyby, Science 321 (2008) 92–94.
[32] R.M. Killen, et al., Observations of metallic species in Mercury's exosphere, Icarus 209 (2010) 75–87.
[33] M.T. Zuber, et al., Laser altimeter observations from MESSENGER's first Mercury flyby, Science 321 (2008) 77–79.
[34] D.E. Smith, et al., The equatorial shape and gravity field of Mercury from MESSENGER flybys 1 and 2, Icarus 209 (2010) 88–100.
[35] B.J. Anderson, et al., The structure of Mercury's magnetic field from MESSENGER's first flyby, Science 321 (2008) 82–85.
[36] H. Uno, et al., Modeling Mercury's internal magnetic field with smooth inversions, Earth Planet. Sci. Lett. 285 (2009) 328–339.
[37] B.J. Anderson, et al., The magnetic field of Mercury, Space Sci. Rev. 152 (2010) 307–339.
[38] J.A. Slavin, et al., Mercury's magnetosphere after MESSENGER's first flyby, Science 321 (2008) 85–89.
[39] J.A. Slavin, et al., MESSENGER observations of magnetic reconnection in Mercury's magnetosphere, Science 324 (2009) 606–610.
[40] J.A. Slavin, et al., MESSENGER observations of extreme loading and unloading of Mercury's magnetic tail, Science 329 (2010) 665–668.
[41] M.E. Perry, et al., Measurement of the radius of Mercury by radio occultation during the MESSENGER flybys. Planet. Space Sci. 59 (2011) 1925–1931.
[42] J.L. Margot, et al., Large longitude libration of Mercury reveals a molten core, Science 316 (2007) 710–714.
[43] M.T. Zuber, et al., The geophysics of Mercury: current status and anticipated insights from the MESSENGER mission, Space Sci. Rev. 131 (2007) 105–132.
[44] S.J. Peale, et al., A procedure for determining the nature of Mercury's core, Meteorit. Planet. Sci. 37 (2002) 1269–1283.
[45] S. Stanley, et al., Thin shell dynamo models consistent with Mercury's weak observed magnetic field, Earth Planet. Sci. Lett. 234 (2005) 27–38.
[46] U.R. Christensen, A deep dynamo generating Mercury's magnetic field, Nature 444 (2006) 1056–1058.
[47] R. Vilim, et al., Iron snow zones as a mechanism for generating Mercury's weak observed magnetic field, J. Geophys. Res. 115 (2010) E11003, http://dx.doi.org/10.1029/2009JE003528.